機能光断像画像j去によるミクロンレーベル脳機能マッピングー電気生理学との相関研究

機能光断像画像法によるミクロンレーベル脳機能マッピング
― 電気生理学との相関研究

Mapping of Brain Functions at Micron Level with Functional Optical Coherence Tomography – a Correlation Study with Electrophysiological Recordings

Uma Maheswari Rajagopalan* and Manabu Tanifuji**

Abstract

Mapping of the surface activity from various sensory areas of brain has been widely done using optical intrinsic signal imaging (OISI). OISI by the process of detection itself gives integrated information across a depth of a few hundred microns. As a complementary technique, to obtain depth resolved functional maps we have employed functional optical coherence tomography (fOCT). Light scattering changes occurring under neural activity can be used as a probe to obtain depth resolved activity maps. Our earlier research showed that fOCT can reveal the presence of a layer specific activation across the depth of cat visual cortex. Further, we showed that the depth integrated fOCT agrees with the intensity variation of OISI. In this study, we have conducted a comparison of the depth profiles of the depth resolved functional maps with the evoked electrical activity profiles obtained from discrete points using electrophysiological recordings and we found a fairly good agreement between the two results.

1.Introduction

The activity of the brain is mapped with volumetric techniques such as fMRI (functional magnetic resonance imaging) and PET (posotron emission tomography) and they provide a spatial resolution of around a few mm[1]. As a complementary technique that can give functional maps at a higher resolution in animal models is optical intrinsic signal imaging (OISI)[2]. This technique measures the reflectance changes from the cortex and it has revealed organization of functional modules called columns where neurons with similar response properties are clustered together and have dimensions of around a few hundred microns[3-5]. OISI has also provided some valuable insights in understanding the representations of sensory information in the brain[6-9].

OISI rely on the measured reflected light that is actually integration of reflections from depths determined by the collection optics. In contrast, anatomically most of the cortex is layered organization usually in six layers distinguished by cell types and density of cells. Each layer with the cellular responses being not necessarily the same has specific input and output patterns[10]. In OISI, neural activity evoked secondary metabolic changes that are averaged over these layers are mapped. In order to overcome this drawback, we have been employing the novel imaging technique of functional optical coherence tomography (fOCT) to visualize depth resolved functional structure of cat visual cortex[11-13]. We showed in our earlier study[13] that the integrated fOCT results show fairly good correlation with the conventional OISI results. In this study, we have further confirmed the potential of fOCT through comparison of the fOCT depth profiles with the profiles of evoked responses obtained from a number of nearby neurons also called multiunit activitity (MUA) recordings at different discrete depths.

OCT is an optical imaging technique where light from a low coherent source is focused onto the tissue and reflectivity of the internal microstructures at different depths is measured by an interferometer[14]. OCT has been successfully employed for structural imaging of eye and non-neuronal tissues such as skin and gastrointestinal tissues[15]. Recently, its potential in mapping functional signals in the brain and retina has been recognized[16-23] and many groups have started to employ OCT for functional imaging in functional imaging studies. We

* Faculty of food and nutrition sciences

** Integrative Neural systems Lab., Brain Science Institute, Riken

have also been investigating the functional imaging of OB of rat.

2. Methods

2.1 Experimental system

We used a fiber based time-domain OCT imaging system consisting of a Mach-Zehnder type heterodyne interferometer with the basic details found in ref. 13 (Figure 1). The sample arm viewing the animal side consisted of an objective lens of numerical aperture 0.08 and also fitted with a CCD camera. This allowed simultaneous viewing of the cortical surface with the introduction of visible light from an auxiliary laser source (wavelength 680 nm). The whole unit was mounted on a manipulator unit that has five degrees of freedom of translation along three axes and rotation and tilt. The flexibility was needed for making the probing light beam normal to the cortical surface. Galvano scanners were installed so as to perform surface scans. The animal related fluctuation in the signal could be reduced by conducting measurements in synchronization with the heartbeat and respiration and keeping the brain surface immobile by using agarose.

2. 2 Animal and surgery details

Cat was anesthetized with a mixture of 70% N_2O and 30% O_2 supplemented with 1-2% isoflurane and paralyzed with Pancuromium bromide (0.1mg/Kg/hr). The animal was artificially ventilated by a respirator unit. Contact lenses were fitted to eyes to protect cornea from drying. The pupils of the eyes were dilated with 0.5 % tropicamide and 0.5 % phenylephrine hydrochroride. The head of the animal was held tightly by attaching to a metal rod. A stainless steel chamber (18 mm inner diameter) was fixed onto the skull with dental acrylic cement by aseptic surgery. After removal of dura matter, inside of the chamber was filled with 1.2 % agarose and was sealed tightly with a round glass cover slip. Rectal temperature, ECG and expired CO_2 were continuously monitored during both OCT experiments and surgery. The experimental protocol was approved by the Experimental Animal Committee of the RIKEN Institute that follows the guidelines of the National Institute of Health.

2.3 Scan details

The stimuli were the same as that used for OISI and consisted of square-wave gratings (white = 8 cd/m^2, black=0 cd/m^2) having a spatial frequency 0.15 cycle/degree and moving at a velocity of 4 degrees / sec. The stimulus set consisted of five patterns with control or blank (mean luminance 4 cd/m^2), horizontal (0°), vertical (90°) and oblique gratings (45°,135°) and were shown in a random order. All stimuli were generated with a VSG2/3 graphics video board (Cambridge Research Systems, UK). The distance of the CRT screen (200-300mm) was adjusted to have the best focus of optic disks and surrounding vessel patterns.

A total of 40 trials had been obtained for each stimulus. The stimulus presentation and data acquisition were done at the following 2 timings: In the first paradigm (Figure 2), for a single trial, data acquisition was done for 8 sec. Within the 8 sec interval, 16 x-z frames (128 x100 pixels) were obtained. Inter-stimulus interval (ISI) was 5 sec. The scanning depth fixed as 1 mm was sampled at 10 μm and speed was 2mm/sec.

In the second paradigm, a single trial took 12 sec and ISI was 10sec and scan depth was 1.5mm and scan speed was 1.5 mm/sec. Within the duration of 12sec, 12 x-y-z frames (660x3x100 voxels with the corresponding scan region being 2 x 0.4x 1.5 mm^3) were obtained and averaged over y-frames. For both cases, stimulus appeared with a delay of 2 sec after the acquisition onset and persisted for 2 sec.

2.4 OISI recording details

Prior to doing functional imaging with OCT, we performed optical intrinsic signal imaging (OISI) with the exposed cortical surface of a cat visual cortex in vivo. OISI was done with the same stimulus set of four different oriented gratings and the control or blank screen. OISI revealed that neurons responding to the same orientation

are clustered to form an orientation map across the cortical surface. To record optical intrinsic signals, the exposed cortex was illuminated with light from an incoherent white light source with filter at a wavelength of 607 nm. The reflected light was imaged onto a commercial CCD camera by a tandem lens system to be analyzed for stimulus evoked reflectance changes.

2.5 Electrophysiology recording details

We recorded average spiking activity of multiple neurons from the recording volume. For that purpose, we used glass coated tungsten electrodes. The electrodes had a tip angle of 5-7.5 degrees and a shank diameter of 70μm. The electrode penetration was done perpendicular to the cortical surface with the blood vessel patterns as the landmark. The electrode was advanced slowly along the cortical depth until the first spiking activity was observed and the corresponding position was considered as the zeroth depth position. We recorded neuronal activities at every 100μm step. At each recording depth, a waiting time of 30min was given to make sure that the electrode positions were stabilized.

The raw electrical signals from the electrode were amplified and low-pass filtered (filter range 0.5 to 10kHz) which were then digitized at 25 kHz. The filtered signals were recorded for 1.5 sec in each trial with the stimulus appearing after 0.5 sec of onset of the trial. The stimulus duration was 0.5sec. ISI was set to be 6sec. A total of 9 different orientations from 0 degrees– 180 degrees of the grating pattern was used as stimuli and presented in a random fashion. 20 trials were done for each stimuli. Square-wave gratings (white = 8 cd/m^2, black=0 cd/m^2) did have the same parameters as that used for OISI and OCT.

We extracted multiple unit activities (MUA) from the filtered signals when it exceeded a certain threshold. The threshold was set as four times the standard deviation of the background noise. Evoked MUA response was calculated as a difference between the mean fire rate obtained during 500ms before stimulus onset to that obtained during the stimulus period.

3. Results

3.1 OCT structural results

Figure 2A shows the difference maps shown in grey scale obtained when horizontal and vertical grating visual stimuli were presented to the cat. Dark and bright regions indicate the activated regions for horizontal and vertical gratings, respectively. OCT x-z scan was done across the line indicated in the OISI map and shown in Figure 2B. Bright regions indicate the scattering centers within the cortex. Here, the light beam was adjusted to be incident normal to the cortical surface and at a position of interest in relation to the cortical surface.

3.2 OCT data analysis

For a single stimulus, we obtained a total of 640 x-z scans. Following procedure was applied to all the collected images before calculating the functional maps:

1. The scans were corrected for the misalignment of the surface position a correlation based procedure used previously[12];
2. Pixel noise was removed with a smoothing filter of window size 3x3;
3. Scaled for nonlinearity between the forward and backward z-scans.

Next, the ratio of the post-stimulus over pre-stimulus scans were calculated for all the grating stimuli and the control condition as follows:

$$\gamma_s(x,d,t) = \frac{R_s^{post}(x,d,t)}{\sum_{prescans} R_s^{pre}(x,d,t)} \quad . \tag{1}$$

Here R_s is the reflectivity at position (x,d) at time t. *post* and *pre* indicate the post-stimulus and pre-stimulus scans. Next, the ratio was averaged for all the scans obtained for each stimulus $\langle \gamma(x,d) \rangle$. Finally, the differential OCT signal $\gamma_{diff}(x,d)$ was calculated as,

$$<\gamma_{diff}(x,d)>=<\gamma_{grating}(x,d)>-<\gamma_{control}(x,d)>. \qquad (2)$$

With the above equation by subtracting the differential OCT signal of the control, noise fluctuations such as respiration artifact that were locked to the recording, but not to the grating stimulus were removed. In this discussion, we restrict ourselves mainly to the results obtained from calculating the difference between $<\gamma(x,d)>$ that were obtained for two orthogonal gratings. The spatial map were smoothened with a moving average filter of size around 100μm x 115μm.

3.3 fOCT results

Figure 4 shows the calculated fOCT maps obtained as a difference of the fOCT maps of horizontal and vertical grating stimuli from OCT scans of Fig. 3. Here, red and blue patches indicate the activation for horizontal and vertical grating stimluli, respectively. From the fOCT maps shown, we can make the following inferences:

1. There is a discrete distribution of activation patches across depth and is stimulus specific;
2. In the very superficial region of less than 100-200μm, there are no activation patches indicating layer 1 where neurons are scarce;
3. In the region deeper than 100-200 μm, there exists several localized patches across depth showing no regular structure;
4. The localized patches extend up to the measured depth of around 1 mm;
5. This indicates that across depth there might exist an organization more complex than the commonly believed continuous cylinder like organization of Hubel and Wiesel[10].

   To address the question of what these patches represent, whether they represent a localization in the distribution of neurons themselves or the localization of the secondary mechanisms that are behind the origin of the functional signals, we performed the following:

1. Comparison of the integrated OCT profile with the OIS intensity variation across the scanned region to find out the correlation with the surface maps obtained by OISI[13]. In that study we could show the existence of fairly high correlation;
2. Comparison of fOCT signals with electrophysiological recording of multi-unit activities (MUA) at the scanned region.

3.4 Comparison of fOCT results with integrated OISI results

As the correlation of OISI maps with neural activity is already well established (3, 4, 41), a comparison of fOCT with OISI is a reasonable validation approach and was was reported earlier[13]. We compared the intensity variation of an OISI map across the scanned line (Fig. 3) with the integrated profile of fOCT (Fig. 4). In order to calculate the integrated profile, all the pixels across the z-direction were summed to obtain a profile that varies only across x; then the differential OCT signal at each lateral position x was calculated. An example of such comparison with the red line indicating the integrated result and green line indicating the OIS intensity variation is shown in Fig. 5. A clear and remarkable agreement between the profiles can be seen. This indicates that fOCT signal is indeed correlated with OISI and thus correlated with the neural activity.

Experiments were done in 5 cats and showed a good correlation between the integrated fOCT signal and the intensity profiles obtained from intrinsic maps. Correlation coefficients vary in the range of 0.3–0.9. However, a general caveat is that there are many differences between OISI and fOCT, including illumination and detection geometries, wavelengths used and the origin of the signals. In fOCT, as near-infrared wavelength is used, oxy- and deoxy-hemoglobin have almost the same absorption coefficients and hence the absorption changes are minimal. The main

source of the signal is thought to be scattering changes. Nevertheless, the OISI results corresponded very well with the integrated profiles of fOCT .

3.4 Comparison of fOCT results with multi-unit activities (MUA)

Next, to investigate what the patches in fOCT maps represent, we recorded multi-unit activities (MUA) in the scanned region to determine the correlation with the distribution of strength of neuronal activity. We compared the depth profiles obtained from the functional maps with the multi-unit activities recorded from a few tracks (S1 to S4) along the recorded line indicated by the red lines in Figs. 3 &4. Figure 6 shows the results of variation of MUA with respect to the cortical depth for four different grating orientations from four different tracks as indicated by the dark filled circles on the line of scan in Fig. 3. As can be seen, for a single track, the stimulus selectivity across that track is preserved. However, the evoked response at different depths is not of the same magnitude and it varies across depth with the response being the largest for 100-400μm. This implies that across depth all neurons do not behave in the same way and they have individual differences as one would expect. We would like to emphasize this variation in the evoked response and we expect this variation could be detected by the proposed fOCT measurement.

Figure 7 shows the results of comparison of the fOCT depth profiles across the tracks of Figs. 3& 4. The fOCT profiles agreed fairly with that of the non-uniformity of evoked response across depth. This indicates that the functional signal measured by fOCT could be correlated with the spiking activity of neurons. The electrode positions were estimated using the blood vessels as landmarks and these may lead to considerable room for errors in localizing the electrode position with respect to the scan line. So to improve the localization, fOCT maps were obtained from an averaged area instead from a single scan line. The scan paradigm has been modified so as to scan along y-axis over an area of 200μm and collapse all the x-y-z scans to a single x-z scan as described in the methods section 2.3.

Figure 8 shows respectively the result of y-averaged x-z fOCT differential map from an area indicated in the OIS intensity map for horizontal and vertical grating (A) and oblique gratings 45 and 135 degrees (B). The black dots within the green demarcated region indicate the six different electrode positions. In the fOCT map, the activated regions appear as red.

Next, we compared the profile of the evoked response across the tracks shown within the delineated region and the corresponding averaged fOCT depth profiles across those tracks. Figure 9 shows for two differential cases of 0deg-90deg and 45deg-135deg from six different sites. As can be seen, the profiles agreed fairly well. A calculation of the correlation coefficient revealed that the profiles were interrelated well. Results of correlation obtained from six different scan positions and three different cats are presented in Table 1 A and B, respectively. Except for two cases, the correlation coefficient is relatively high and hence proving that fOCT could indeed measure functional maps.

Summary

We demonstrated that OCT technique, which is mainly used for performing structural observation, can be successfully implemented to investigate functional organization of brain. Our OCT system was used to obtain depth resolved layer specific information from visual cortex and is theoretically capable of resolving functional structures up to 17 mm in the depth direction. The depth resolution is mainly limited by the coherence length of the source. Using a source that has a broader spectrum will lead to a higher resolution as well as reduce the effect of speckles. Speckles are characteristic phenomena that appear when the coherency of light increases and are due to the interference of multiply scattered light from a turbid medium like brain. It is worth to point out that the result of a single OCT scan contains the effect of speckles. These speckles (also called biospeckles) are dynamic due to the random motion of scatterers within the tissue. Temporal averaging greatly reduces the effect of the

speckles and, therefore, the averaged results presented in Fig.3. Fig. 4B, and 8A and B with speckles averaged out.

Our proposed novel technique for conducting functional imaging of brain can operate in a complementary way to the widely used and well established single electrode studies and the currently emerging OISI techniques. The former is a single point direct measurement of single neuro activity and can measure discretely across the whole depth and is not capable of mapping the activity from a network of multiple neurons. In contrast, the OISI is an indirect technique capable of mapping the activity simultaneously at micron level resolution from multiple neurons but has the limitation of probing across the depth. Finally, in conclusion, we expect fOCT to be a promising technique capable of delivering results on the working of the brain not only at the cellular but also at the level of network organization.

It should be mentioned that in the comparison study discussed in the 3.5, different methods of OISI, fOCT and MUA were conducted independently to be compared later. However, there could be some spatial ambiguity of 100 μm or more in such comparisons. For more reliable comparisons, it may be necessary to conduct simultaneous measurements of OISI, fOCT and MUA. In addition, recently, we have started the implementation of a high speed swept source OCT system that would largely improve the sensitivity of OCT signal enabling a clearer picture of the columnar organization of orientation columns in cat visual cortex[23].

Recently, we have also started applying fOCT to the study of the rat olfactory system and our preliminary results show clear odor-dependent responses (unpublished). We therefore expect this method to provide novel insights regarding the response distribution in granule cell layers that receive input from olfactory glomeruli and lie deeper from superficial regions of the bulb.

Acknowledgements

MT was supported by Grant-in-AID for Scientific Research 22300137, 26240021 from the Ministry of Education, Culture, Sports, Science, and Technology (MEXT). MT was also supported by Grant-in-AID for Scientific Research on Innovative Areas, "Sparse Modeling" (25120004) from MEXT, Japan.

References

1. Toga and J.C.Mazziotta, *Brain mapping-The methods* (Academic press, New York) 1996.
2. D. Y. Ts'o, R.D.Frostig, E.E.Leike and A.Grinvald, Science **249** (1990) 417.
3. T.Bonhoeffer and A.Grinvald, J.Neurosci., **13** (1993) 4157.
4. 谷藤 学、応用物理 **68** (1999) 997.
5. D.Malonek, R.B.H.Tootell and A.Grinvald, Proc.R.Soc.Lond.B **258** (1994) 109.
6. G.Wang,K.Tanaka,M.Tanifuji, Science **272** (1996) 1665.
7. G.Wang, M.Tanifuji, K.Tanaka, Neurosci.Res., **32** (1998) 33.
8. N.Uchida,Y.K.Takahashi,M.Tanifuji, K.Mori, Nature Neurosci., 3 81035) 2000.
9. K.Tsunoda,Y.Yamane,M.Tanifuji, Nature Neurosci., **4** (2001) 832.
10. D.H. Hubel and T.N.Wiesel, J.Neurophysiol., **28** (1965) 229. ibid, Ferrier lecture, Proc.Roy.Soc.London B **198** (1977) 1.
11. R. U. Maheswari, H. Takaoka, R. Homma, H. Kadono, M. Tanifuji, "Implementation of optical coherence tomography (OCT) in visualization of functional structures of cat visual cortex," Opt. Commun. **202**, 47-54 (2002).
12. R. Uma Maheswari, H. Takaoka, H. Kadono, R. Homma, M. Tanifuji, "Novel functional imaging technique from brain surface with optical coherence tomography enabling visualization of depth resolved functional structure in vivo" J. Neurosci. Meth **124,** 83-92 (2003).
13. Uma Maheswari Rajagopalan, Manabu Tanifuji, "Functional Optical Coherence Tomography reveals localized layer specific activations in cat primary visual cortex in vivo", Opt. Lett., **32**, 2614-2616 (2007).
14. D. Huang, E. A. Swanson, C. P. Lin, J. S. Schuman, W. G. Stinson, W. Chang, M. R. Hee, T. Flotte, K. Gregory, C. A. Puliafito, J. G. Fujimoto, "Optical coherence tomography," Science **254**(5035), 1178-1181 (1991).

15. M. Wojtkowski, "High-speed optical coherence tomography: basics and applications," Appl. Opt. **49**(16), D30-D61 (2010).
16. S. A. Boppart, B. E. Bouma, C. Pitris, J. F. Southern, M. E. Brezinski, J. G. Fujimoto, "In vivo cellular optical coherence tomography imaging," Nat. Med. **4**(7), 861-865 (1998).
17. J. G. Fujimoto, "Optical coherence tomography for ultrahigh resolution in vivo imaging," Nat. Biotechnol. **21**(11), 1361-1367 (2003).
18. K. Tsunoda, K. Fujinami, Y. Miyake, "Selective abnormality of cone outer segment tip line in acute zonal occult outer retinopathy as observed by spectral-domain optical coherence tomography," Arch. Opthalmol. **129**(8), 1099-1101 (2011).
19. Y. Muraoka, H. Ohashi Ikeda, N. Nakano, M. Hangai, Y. Toda, K. Okamoto-Furuta, H. Kohda, M. Kondo, H. Terasaki, A. Kakizuka, N. Yoshimura, "Real-time imaging of rabbit retina with retinal degeneration by using spectral-domain optical coherence tomography," PLoS ONE **7**(4), e36135 (2012).
20. A. D. Aguirre, Y. Chen, J. G. Fujimoto, "Depth-resolved imaging of functional activation in the rat cerebral cortex using optical coherence tomography," Opt. Lett. **31**(23), 3459-3461 (2006).
21. Y. Chen, A. D. Aguirre, L. Ruvinskaya, A. Devor, D. A. Boas, J. G. Fujimoto, " Optical coherence tomography (OCT) reveals depth-resolved dynamics during functional brain activation," J. Neurosci. Methods **178**(1), 162-173 (2009).
22. V. J. Srinivasan, S. Sakadžić, I. Gorczynska, S. Ruvinskaya, W. Wu, J. G. Fujimoto, D. A. Boas, "Depth-resolved microscopy of cortical hemodynamics with optical coherence tomography," Opt. Lett. **34**(20), 3086-3088 (2009).
23. Y. Nakamichi, V. A. Kalatsky, H. Watanabe, U. M. Rajagopalan, M. Tanifuji, "3D structure of the orientation column in cat primary cortex revealed by functional optical coherence tomography," Abstr. Soc. Neurosci. **270.01** (2011).

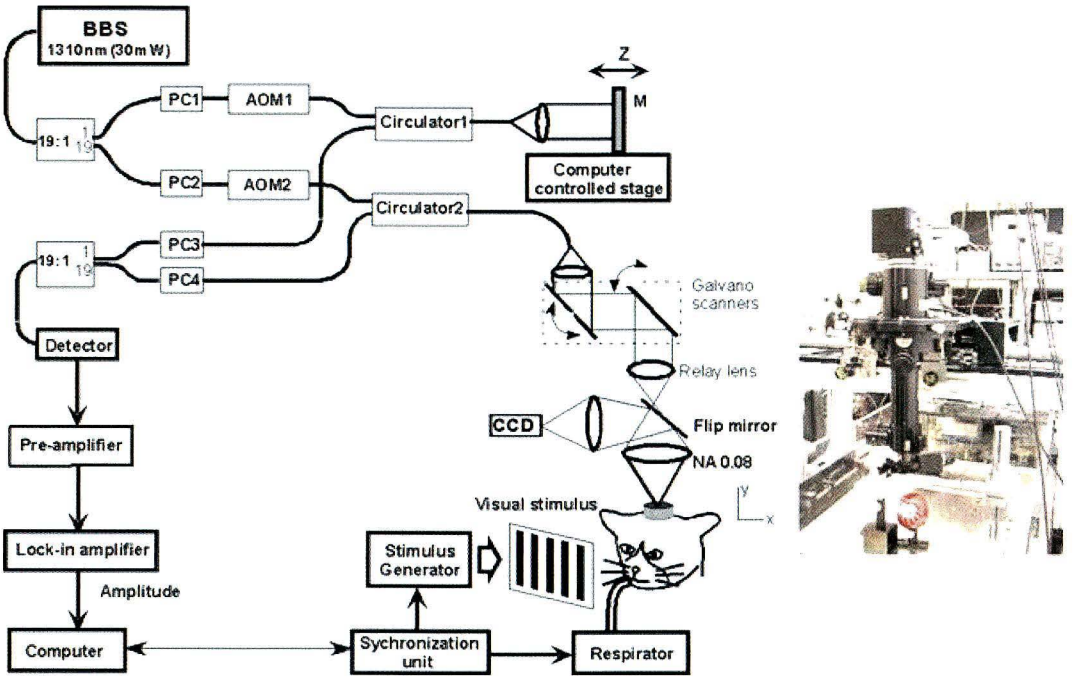

Figure 1. A schematic of the experimental system (A) with a picture of the probe (B). In figure (A), the abbreviations denote: BBS – Broad Band Source, AOM- Acousto-Optic Modulator, PC - Polarization Controller, M – Mirror and O – Objective lens.

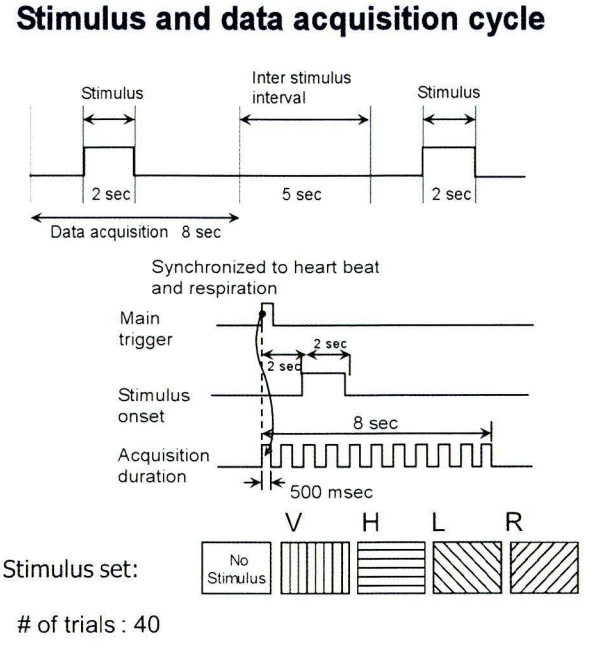

Figure 2. Stimulus presentation protocol with the types of grating stimuli of the commonly used paradigm in the experiments.

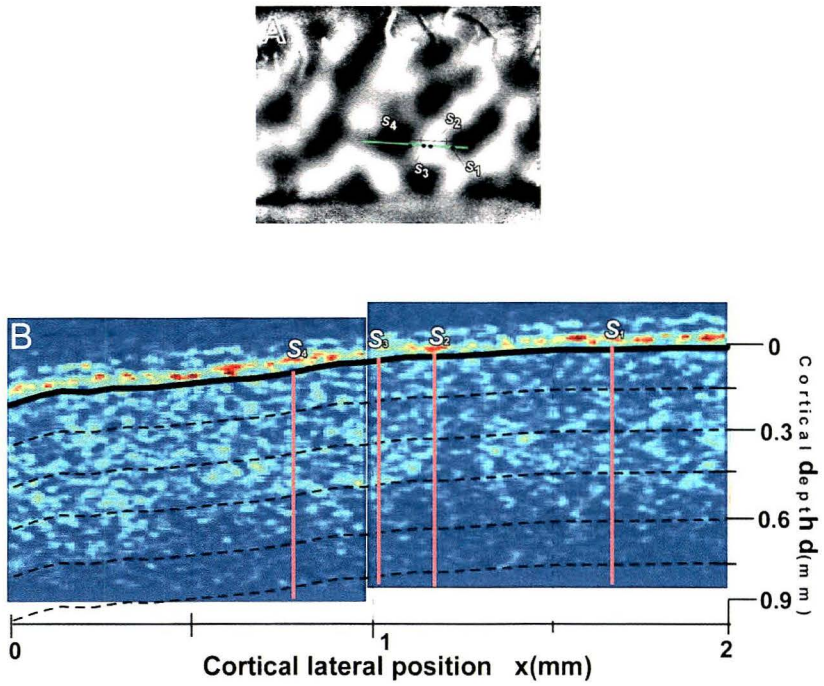

Figure 3. OISI result (A) along with the OCT structural image (B) obtained across the green line in (A). The OISI image (A) was obtained from the difference of intrinsic activation maps between horizontal and vertical grating stimuli. S1 to S4 indicate the electrode penetration sites.

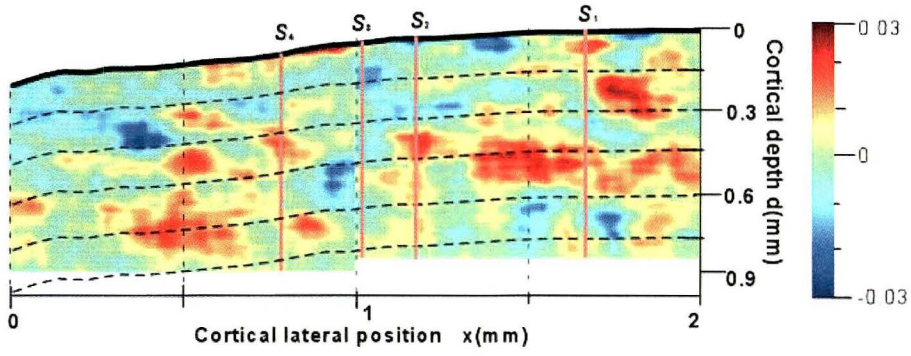

Figure 4. Calculated fOCT horizontal minus vertical difference map of OCT scans of Fig.2.

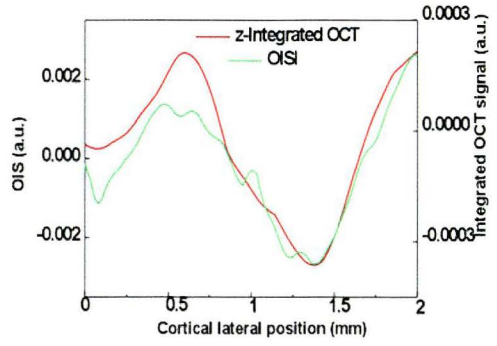

Figure 5. Comparison of z-integrated fOCT of Fig.4 with the variation of intensity across the line in OISI of Fig.3.

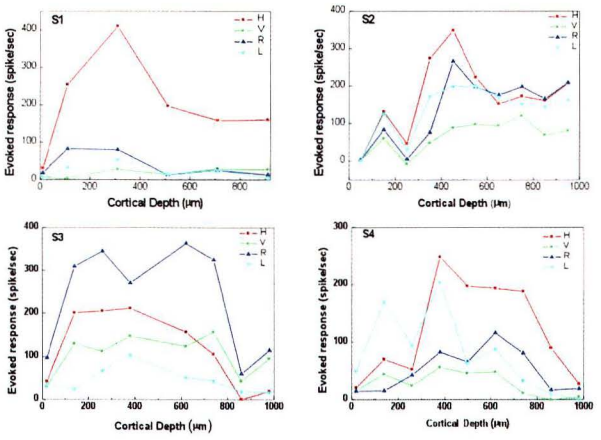

Figure 6. Evoked response across the four electrodes S1 to S4 sampled at at every 100μm

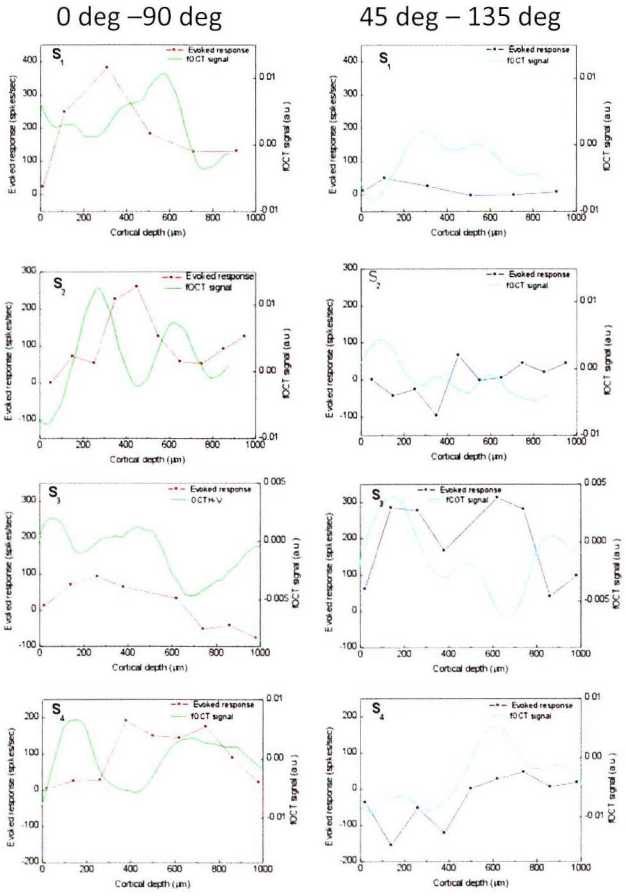

Figure 7 Evoked response with the respective fOCT signals obtained across the tracks S1 to S4 for orthogonal stimuli for 0deg miuns 90 deg (left) and 45 deg minus 135 deg (right). In the graphs, red and green indicate respectively the fOCT signal and the evoked response for 0 deg-90 deg . Cyan and blue respectively indicate the fOCT signal and the evoked response for 45 deg-135 deg .

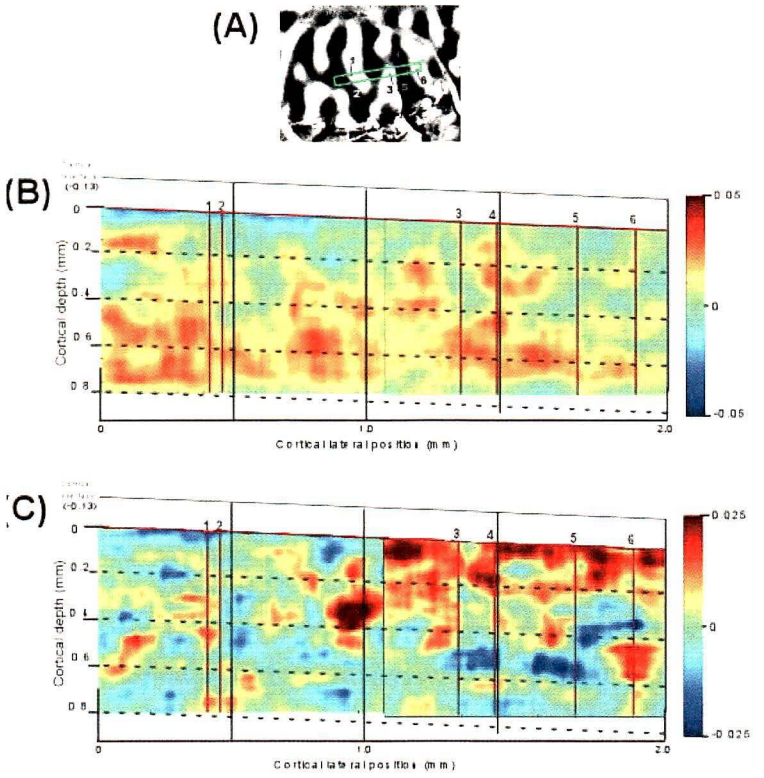

Figure 8. fOCT x-z maps for 0 deg – 90 deg (B) and 45 deg – 135 deg (B) with cortical surface map (A) with the scan region indicated by the green line and the electrode penetration sites indicated by dots.

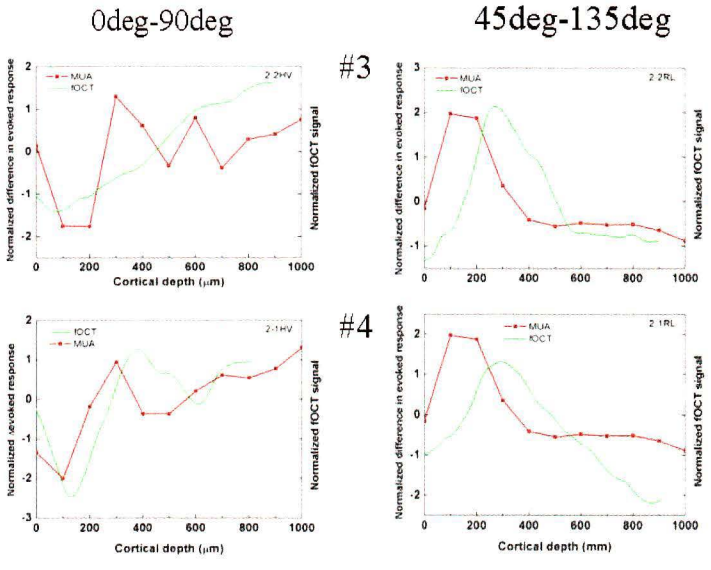

Figure 9. Evoked response against the cortical depth along with the corresponding fOCT response obtained from two different sites # 3 and # 4 for 0 deg-90 deg (left) and 45 deg – 135 deg (right). Here red indicates the discrete evoked response and green indicates the continuous functional OCT signal.

Site #	Correlation coeff. for 0-90 deg	Correlation coeff. for 45-135
#1	0.94	0.66
#2	0.809	0.764
#3	0.908	0.926
#4	0.852	0.899
#5	0.348	0.374
#6	0.751	0.365

Table 1 Correlation coefficient between the evoked response and the functional OCT signal from six different sites for 0 deg minus 90 deg and 45 deg minus 135 deg.

Cat #	# of sites that show significant correlation ($p<0.005$)
C-22	4/8
C-30	9/11
C-36	5/11

Table 2 Number of electrode penetration sites that showed significant correlation between the evoked response and the corresponding fOCT signal from three different cats.